for $PhCH_2Cl$ and 3.0×10^{-4} M^{-1} s^{-1} for *n*-BuBr. Clearly a different explanation for these seemingly conflicting findings is needed. The products were found to be different; benzyl chloride reacted with the cobalt(I) complex to yield the expected benzyl derivative, whereas the π CH_2=CHCN adduct also gave appreciable quantities of the inorganic cobalt(III) complex, chlorocobaloxime. Thus a halide ion abstraction mechanism seems to intervene in this case.

Discussion

The earlier assignments of a five-coordinate structure to Co(I) cobaloxime complexes seem well supported by the large changes in the spectra of Co(I) cobaloxime complexes in solutions containing different bases. Further, coordination of five ligands to a d^8 ion would give rise to an 18-electron configuration giving stability to a geometry which is generally visualized as only a transition state in the chemistry of octahedral and square-planar complexes. The observed kinetic rate law for at least the reactions of CH_2CHCN and CH_3S^- rules out a simple bimolecular mechanism involving a geometry of higher (6) coordination number. On the other hand, the rate law is consistent with an intermediate of reduced coordination number.

We note that the values of k_5/k_{-4} for CH_3S^- and CH_2CHCN are rather close, 0.59 and 0.19, supporting the mechanism of eq 4–8. Also, as remarked earlier, the constancy of k_4 between the three systems provides supporting evidence as well.

The observation that $[Co^I(dmgH)_2P(C_4H_9)_3]^-$ and $[Co^I(dmgH)(dmgBF_2)P(C_4H_9)_3]^-$ react with CH_2=CHCN faster than $[Co^I(dmgBF_2)_2P(C_4H_9)_3]^-$ by factors of 25–40 and 10–20, respectively, is consistent with a dissociative process. (These rates reflect variations in k_4.) With greater delocalization of the electron density in the equatorial ligands, the dissociation rate of the $[Co^I-P(C_4H_9)_3]^-$ bond decreases. In view of the 18-electron configuration, it is not surprising that a 16-electron transition state seems more favorable.

Another notable finding is that while CH_3CH_2CN does not form complexes with $[Co^I(dmgBF_2)_2P(C_4H_9)_3]^-$, the olefinic analogue CH_2=CHCN forms relatively stable complexes and competes very favorably for the four-coordinate intermediate as seen for k_5/k_{-4} (Table III). Were the C≡N group the ligating site in CH_2=CHCN, it would be difficult to account for (a) the much greater stability of the acrylonitrile adduct as compared to that with CN^- (K > ca. 10^3 vs. K = 0.37) and (b) the much more effective competition of CH_2=CHCN than of CN^- for the four-coordinate intermediate, 0.59 vs. 0.011 for k_5/k_{-4}.

On the basis of our kinetic data and other evidence, it is reasonable to conclude that the five-coordinate $Co^I(dmgBF_2)_2P(C_4H_9)_3$ reacts with CH_2CHCN, CN^-, and CH_3S^- by a dissociative mechanism to give products with different degrees of π bonding. The reactions of Co^I acrylonitrile adducts with H^+ should be of considerable interest from the point of view of the mechanisms of homogeneous hydrogenation processes.

Acknowledgment. This work was supported by the U.S. Department of Energy, Contract No. W-7405-Eng-82, Office of Basic Energy Sciences, Division of Chemical Sciences, budget code AK-01-03-02-1.

Registry No. $ClCo(dmgBF_2)_2P(C_4H_9)_3$, 73117-41-6; $ClCo(dmgBF_2)(dmgH)P(C_4H_9)_3$, 73117-42-7; $ClCo(dmgBF_2)_2C_5H_5N$, 73117-43-8; $[Co^I(dmgH)_2P(C_4H_9)_3]^-$, 63902-69-2; $[Co^I(dmgH)(dmgBF_2)P(C_4H_9)_3]^-$, 73117-26-7; $[Co^I(dmgBF_2)_2P(C_4H_9)_3]^-$, 73117-27-8; $[Co^I(dmgBF_2)_2C_5H_5N]^-$, 31319-33-2; $[Co^I(dmgBF_2)_2(CH_2$=CHCN)]$^-$, 73117-28-9; CH_2CHCN, 107-13-1; CH_3S^-, 17032-46-1; CN^-, 57-12-5; $ClCo(dmgH)_2P(C_4H_9)_3$, 24501-27-7; $PhCH_2Cl$, 100-44-7; *n*-BuBr, 109-65-9; $ClCo(dmgH)_2C_5H_5N$, 23295-32-1.

Contribution from the Department of Chemistry, Florida Atlantic University, Boca Raton, Florida 33431

Electrochemistry of Aqueous Molybdenum(VI), -(V), and -(III) Catechol Complexes. Dimerization of Molybdenum(V) in Weakly Acidic Solution

LYNN M. CHARNEY and FRANKLIN A. SCHULTZ*

Received October 9, 1979

Electrochemical reduction of the *cis*-dioxo molybdenum(VI)–catechol complex, $MoO_2(cat)_2^{2-}$, in pH 3.5–7 aqueous buffers occurs by sequential one- and two-electron transfers to yield transiently stable Mo(V) and Mo(III) species, $MoO(H_2O)(cat)_2^-$ and $Mo(H_2O)_2(cat)_2^-$. Uptake of two protons accompanies each electron-transfer step and converts an oxo group to a coordinated water molecule. Pyridine substitution occurs at these aquo sites. Formation constants of the species $MoO(py)(cat)_2^-$, $Mo(H_2O)(py)(cat)_2^-$, and $Mo(py)_2(cat)_2^-$ are determined from voltammetric half-wave potential measurements. The reduced molybdenum monomers are not stable indefinitely at pH <7. Dimerization to the di-μ-oxo species, $Mo_2O_4(cat)_2(H_2O)_2^{2-}$, occurs after reduction to the Mo(V) state. The mechanism of the reaction has been investigated by cyclic voltammetry. The mechanism involves dissociation of one molecule of pyridine and one molecule of catechol from $MoO(py)(cat)_2^-$ to produce a 1:1 molybdenum(V)–catechol monomer, which undergoes dimerization by acid-dependent and acid-independent pathways.

Recent electrochemical studies of molybdenum compounds[1-8] have sought to establish relationships between structural and electron-transfer properties which may prove helpful in understanding the redox behavior of molybdoenzymes. Most of this work has dealt with oxo- or sulfido-bridged molybdenum(V) dimers, which are prevalent structural forms of this oxidation state. However, recent X-ray absorption studies indicate that the active sites of nitrogenase,[9] sulfite oxidase,[10] and xanthine oxidase[11] may be mononuclear

(1) V. R. Ott and F. A. Schultz, *J. Electroanal. Chem.*, **59**, 47 (1975).
(2) V. R. Ott and F. A. Schultz, *J. Electroanal. Chem.*, **61**, 81 (1975).
(3) L. J. DeHayes, H. C. Faulkner, W. H. Doub, Jr., and D. T. Sawyer, *Inorg. Chem.*, **14**, 2110 (1975).
(4) J. K. Howie and D. T. Sawyer, *Inorg. Chem.*, **15**, 1892 (1976).
(5) V. R. Ott, D. S. Swieter, and F. A. Schultz, *Inorg. Chem.*, **16**, 2538 (1977).
(6) G. Bunzey, J. H. Enemark, J. K. Howie, and D. T. Sawyer, *J. Am. Chem. Soc.*, **99**, 4168 (1977).
(7) J. Hyde, K. Venkatasubramanian, and J. Zubieta, *Inorg. Chem.*, **17**, 414 (1978).
(8) F. A. Schultz, V. R. Ott, D. S. Rolison, D. C. Bravard, J. W. McDonald, and W. E. Newton, *Inorg. Chem.*, **17**, 1758 (1978).
(9) S. P. Cramer, K. O. Hodgson, W. O. Gillum, and L. E. Mortenson, *J. Am. Chem. Soc.*, **100**, 3398 (1978).

0020-1669/80/1319-1527$01.00/0

with respect to molybdenum. Monomeric molybdenum species exhibiting reversible electron-transfer properties would be of interest in this regard, but known examples,[12-15] particularly in aqueous solution,[16] are sparse.

As an entry to the redox behavior of monomeric molybdenum complexes in aqueous media, we have investigated the electrochemistry of the well-characterized[17-19] *cis*-dioxo molybdenum(VI) compound, $MoO_2(cat)_2^{2-}$, where cat^{2-} is the catecholate dianion ($C_6H_4O_2^{2-}$). Our attention was drawn to this compound by several recent observations. These include (1) a number a transition metals (Co,[20] Fe,[21] Mn,[22] Cr,[23] Ce[24]) which, when coordinated to catechol, exhibit one or more reversible electron transfers, (2) an interesting variety[25] of recently synthesized molybdenum compounds with catechol or catechol-like ligands, and (3) reports that low-valent molybdenum and vanadium catecholate complexes catalyze the reduction of nitrogenase substrates.[26]

Zelinka et al.[27] carried out a polarographic investigation of $MoO_2(cat)_2^{2-}$ in pH 2–8 buffers. These authors correctly identified the principal reduction mechanism of this compound as sequential Mo(VI) → Mo(V) and Mo(V) → Mo(III) electron transfers. However, they failed to obtain or misinterpreted information regarding compositions, structures, and chemical reactions of the electrode products. We wish to report here the results of a comprehensive study by cyclic voltammetry and controlled-potential coulometry of the electrochemical reduction of $MoO_2(cat)_2^{2-}$ in pH 3.5–7 aqueous buffers. Stabilization by catechol of reversibly reducible monomers affords a unique opportunity to observe structural changes which accompany electron transfer at a monomeric molybdenum center in aqueous media. In particular, it has been possible to detect the binding of ligands (in addition to catechol) at coordination sites made available by reduction of oxomolybdenum groups and to establish a mechanism for dimerization of the monomeric Mo(V) species. During the course of this investigation a well-defined dichotomy in electrochemical behavior, in terms of electrode half-reactions and final chemical products, became apparent between high and low pH values. Consequently, results at pH <7 are presented in this paper and those at pH >7 in a subsequent article.[28]

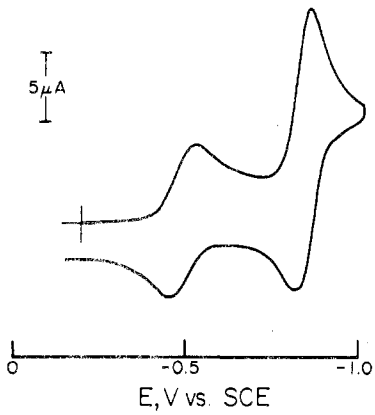

Figure 1. Cyclic voltammogram of $MoO_2(cat)_2^{2-}$ in pyridine buffer: 1mM Mo(VI), 0.10 M H_2cat, 0.02 M pyH^+, 0.18 M py, pH 6.6, sweep rate = 0.2 V s^{-1}.

Experimental Section

Instrumentation. Electrochemical experiments were carried out with instrumentation described previously.[1] The working electrode for voltammetric experiments was a Metrohm E410 hanging mercury drop of 0.0222-cm^2 area and for coulometric experiments was a 12-cm^2 mercury pool. In cyclic voltammetric experiments a fresh mercury drop was used for each trial and was equilibrated with the solution for 30–60 s before measurement. Potentials are reported relative to a saturated calomel (SCE) reference electrode. All voltammetric experiments were conducted in a Brinkmann E615 cell which was thermostated at 25.0 ± 0.1 °C by a circulating water bath.

Infrared spectra were recorded in KBr disks on a Perkin-Elmer 621 spectrophotometer. Elemental analyses were by Galbraith Laboratories.

Materials and Procedures. Practical grade catechol (Eastman) was purified by distillation and recrystallization.[29] The brown practical grade catechol melted into a black liquid which distilled at 185–190 °C by using a house vacuum line. The vapors solidified into white crystals in an ice-cooled collection flask. The catechol was recrystallized twice from toluene and stored under vacuum. All other chemicals were reagent-grade materials.

Solutions were prepared with doubly distilled water and deaerated with argon. The argon was passed successively through gas-washing towers containing chromous chloride solution (twice), distilled water, and the buffer solution of the experiment. Solutions were prepared by first adding catechol to deaerated buffer solution in the electrochemical cell. Avoidance of catechol oxidation was checked by noting the absence of color development in the solution and extraneous peaks in a voltammetric background trace. Otherwise, the solution was discarded. In coulometric experiments the catechol–buffer solution also was prereduced for 30–60 min at the potential of the electrolysis. A weighed portion of solid sodium molybdate was added to the cell to generate the complex.

In near neutral solution Mo(VI) and catechol react to form 1:1 and 1:2 complexes

$$MoO_4^{2-} + H_2cat \rightleftarrows MoO_2(OH)_2(cat)^{2-} \quad \beta_1^{VI} \qquad (1)$$

$$MoO_4^{2-} + 2H_2cat \rightleftarrows MoO_2(cat)_2^{2-} + 2H_2O \quad \beta_2^{VI} \qquad (2)$$

The overall formation constants are $\beta_1^{VI} = 37\ M^{-1}$ and $\beta_2^{VI} = 5.4 \times 10^4\ M^{-2}$ (pH 7.3, $\mu = 0.1$, $T = 25$ °C).[18] With 1×10^{-3} M Mo(VI) present, a 50-fold or greater excess of catechol converts >98% of the Mo(VI) into the 1:2 complex. We nominally used 1×10^{-3} M Mo(VI) and 0.15 M catechol to ensure essentially complete formation of the

(10) S. P. Cramer, H. B. Gray, and K. V. Rajagopalan, *J. Am. Chem. Soc.*, **101**, 2772 (1979).
(11) T. D. Tullius, D. M. Kurtz, Jr., S. D. Conradson, and K. O. Hodgson, *J. Am. Chem. Soc.*, **101**, 2776 (1979)
(12) A. Nieuwpoort and J. J. Steggerda, *Recl. Trav. Chim. Pays-Bas*, **95**, 250 (1976).
(13) J. Hyde and J. Zubieta, *J. Inorg. Nucl. Chem.*, **39**, 289 (1977).
(14) J. K. Gardner, N. Pariyadath, J. L. Corbin, and E. I. Stiefel, *Inorg. Chem.*, **17**, 897 (1978).
(15) R. D. Taylor, J. P. Street, M. Minelli, and J. T. Spence, *Inorg. Chem.*, **17**, 3207 (1978).
(16) P. Chalilpoyil and F. C. Anson, *Inorg. Chem.*, **17**, 2418 (1978).
(17) L. Havelkova and M. Bartusek, *Collect. Czech. Chem. Commun.*, **34**, 2919 (1969); M. Bartusek, *ibid.*, **38**, 2255 (1973).
(18) K. Kustin and S. T. Liu, *J. Am. Chem. Soc.*, **95**, 2487 (1973).
(19) V. V. Tkachev and L. O. Atovmyan, *Koord. Khim.*, **1**, 845 (1975).
(20) P. A. Wicklund and D. G. Brown, *Inorg. Chem.*, **15**, 396 (1976).
(21) S. R. Cooper, J. V. McCardle, and K. N. Raymond, *Proc. Natl. Acad. Sci. U. S. A.*, **75**, 3551 (1978).
(22) K. D. Magers, C. G. Smith, and D. T. Sawyer, *Inorg. Chem.*, **17**, 515 (1978).
(23) S. R. Sofen, D. C. Ware, S. R. Cooper, and K. N. Raymond, *Inorg. Chem.*, **18**, 234 (1979); H. H. Downs, R. M. Buchanan, and C. G. Pierpont, *ibid.*, **18**, 1736 (1979).
(24) S. R. Sofen, S. R. Cooper, and K. N. Raymond, *Inorg. Chem.*, **18**, 1611 (1979).
(25) L. O. Atovmyan, V. V. Tkachev, and T. G. Shishova, *Dokl. Akad. Nauk SSSR*, **205**, 609 (1972); C. G. Pierpont and H. H. Downs, *J. Am. Chem. Soc.*, **97**, 2123 (1975); C. G. Pierpont and R. M. Buchanan, *ibid.*, **97**, 4912, 6450 (1975); C. G. Pierpont and H. H. Downs, *Inorg. Chem.*, **16**, 2970 (1977); R. M. Buchanan and C. G. Pierpont, *ibid.*, **18**, 1616 (1979); J. P. Wilshire, L. Leon, P. Bosserman, and D. T. Sawyer, *J. Am. Chem. Soc.*, **101**, 3379 (1979).
(26) L. A. Nikonova and A. E. Shilov in "Recent Developments in Nitrogen Fixation", W. E. Newton, J. R. Postgate, and C. Rodriguez-Barrueco, Eds., Academic Press, New York, 1977, pp 41–51; A. G. Ovcharenko, A. E. Shilov, and L. A. Nikonova, *Izv. Akad. Nauk. SSSR, Ser. Khim.*, 534 (1975).
(27) J. Zelinka, M. Bartusek, and A. Okac, *Collect. Czech. Chem. Commun.*, **38**, 2898 (1973).
(28) L. M. Charney, H. O. Finklea, and F. A. Schultz, to be submitted for publication.
(29) H. Gilman and A. H. Blatt, Eds., "Organic Synthesis", Collective Vol. I, Wiley, New York, 1941, pp 149–53.

Table I. Voltammetric Data for Reduction of $MoO_2(cat)_2^{2-}$ in Pyridine Buffer[a]

ν, V s^{-1}	$-(E_{1/2})_1$,[b] V	$(\Delta E_p)_1$,[b] mV	$(i_p/\nu^{1/2}AC)_1$,[c] A cm s$^{1/2}$ mol^{-1} V$^{-1/2}$	$(i_{pa}/i_{pc})_1$	$-(E_{1/2})_2$,[b] V	$(\Delta E_p)_2$,[b] mV	$(i_p/\nu^{1/2}AC)_2$,[c] A cm s$^{1/2}$ mol^{-1} V$^{-1/2}$	$(i_{pa}/i_{pc})_2$
0.01	0.486	73	560	0.87	0.834	57	930	0.89
0.02	0.484	69	568	0.89	0.836	44	1050	0.91
0.05	0.482	72	569	0.98	0.836	41	1150	0.93
0.10	0.484	75	564	1.02	0.833	42	1180	0.97
0.20	0.482	73	558	1.03	0.830	49	1200	0.95

[a] Conditions: 1.06 mM Mo(VI), 0.15 M H_2cat, 0.02 M pyH$^+$, 0.10 M py, pH 6.26, μ = 0.5, 25.0 °C. [b] $E_{1/2} = (E_{pc} + E_{pa})/2$, $\Delta E_p = E_{pa} - E_{pc}$. [c] Current parameters corrected for spherical diffusion as described in Table I of ref 32.

$MoO_2(cat)_2^{2-}$ species. Unless noted otherwise, ionic strength was adjusted to 0.5 with sodium sulfate.

Preparation of $BaMo_2O_4(cat)_2(H_2O)_2$. Sodium molybdate dihydrate (7.36 g, 30.4 mmol) and hydrazine dihydrochloride (0.815 g, 7.76 mmol), dissolved separately in 75 and 25 mL of warm 3 M HCl, were mixed and heated until evolution of dinitrogen ceased. Catechol (3.48 g, 31.6 mmol) was added, and the solution was heated gently with stirring for 90 min and then cooled in an ice bath. With the solution still in ice, pH was adjusted to 6.0 with saturated sodium hydroxide. Barium chloride dihydrate (3.68 g, 15.1 mmol), dissolved in a minimum quantity of water, was added with stirring to the molybdenum(V)–catechol solution. The orange precipitate was collected by filtration and washed successively with three portions each of ice-chilled water, ice-chilled acetone, and ether at room temperature. The product was dried at 60 °C. Anal. Calcd for $BaMo_2C_{12}H_{12}O_{10}$: C, 22.33; H, 1.87; Ba, 21.88; Mo, 29.73. Found: C, 20.49; H, 2.82; Ba, 21.24; Mo, 30.10.

The infrared spectrum of the product exhibits strong absorptions at 958 and 936 cm^{-1} which are characteristic of the terminal Mo=O stretching vibrations in $Mo_2O_4^{2+}$ complexes.[5,30] Absorptions at 747 and 477 cm^{-1}, which are of the appropriate frequencies for Mo–O bridge vibrations in this structure, also are observed, but the presence of ligand bands in this region makes the assignments tentative.

Apparently identical compounds having the same molybdenum–catechol stoichiometry were prepared many years ago by Weinland[31] but were not recognized as Mo(V) dimers.

Results

Electrode Half-Reactions. The electrochemistry of $MoO_2(cat)_2^{2-}$ was investigated between pH 3.5 and 7 in formate, acetate, phosphate, and pyridine (py) buffers. Under properly chosen conditions, $MoO_2(cat)_2^{2-}$ exhibits well-defined electrochemistry. Optimal behavior is illustrated in Figure 1; accompanying data are presented in Table I.

The voltammogram in Figure 1 consists of two waves whose relative heights and cathodic-to-anodic peak separations suggest the successive transfer of one and two electrons. At the faster sweep rates in Table I the two waves exhibit the properties of diffusion-controlled reduction ($i_p/\nu^{1/2}AC$ = constant), chemically stable electrode products (i_{pa}/i_{pc} = 1.0), and approximate Nernstian reversibility ($(\Delta E_p)_1$ = 72 mV, $(\Delta E_p)_2$ = 42 mV). The number of electrons transferred in the first wave was determined to be one from controlled-potential coulometry at potentials between $(E_{1/2})_1$ and $(E_{1/2})_2$. For seven trials in pyridine and phosphate buffers, $n = 0.99 \pm 0.12$. At fast sweep rates the ratio of peak current parameters in Table I is $(i_p/\nu^{1/2}AC)_2/(i_p/\nu^{1/2}AC)_1 = 2.15$. Given the somewhat diminished electron-transfer reversibility of the redox couples, this value is reasonably close to the expected ratio[33] $(n_2/n_1)^{3/2}$ = 2.83 for a multistep charge transfer having n_1 = 1 and n_2 = 2. The number of electrons transferred in the second reduction step could not be verified by controlled-potential coulometry at pH 3.5–7, because the product of the first step is not sufficiently stable under these conditions. However, coulometric data obtained at higher pH values[28] show that n_2 = 2. These results confirm the fundamental steps in the reduction of $MoO_2(cat)_2^{2-}$ as Mo(VI) → Mo(V) and Mo(V) → Mo(III) electron transfers.

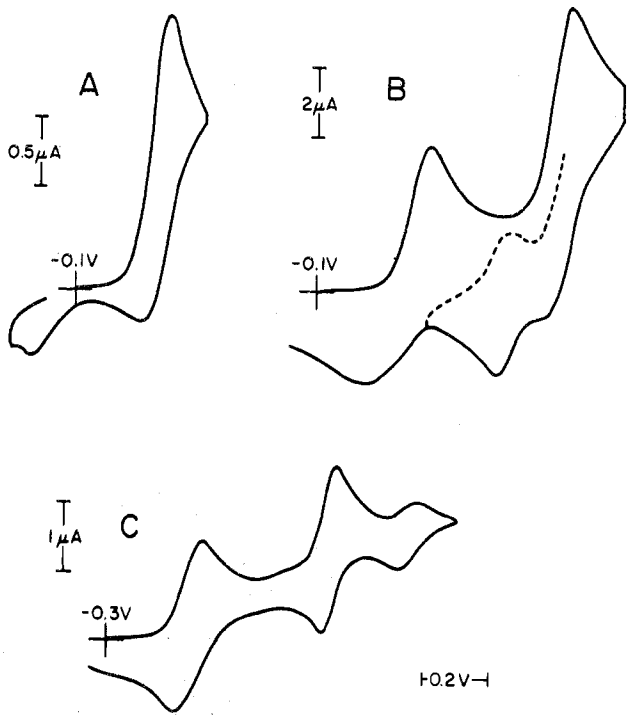

Figure 2. Cyclic voltammograms illustrating nonideal behavior of $MoO_2(cat)_2^{2-}$. All solutions contain 1 mM Mo(VI) and 0.15 M H_2cat: (A) 0.1 M pyH$^+$, 0.01 M py, pH 4.7, sweep rate = 0.01 V s^{-1}; (B) 0.2 M pyH$^+$, 0.2 M py, pH 5.7, sweep rate = 0.1 V s^{-1}; (C) 0.05 M $H_2PO_4^-$, 0.05 M HPO_4^{2-}, pH 6.7, sweep rate = 0.01 V s^{-1}.

Less ideal voltammetric behavior often results if sweep rate is decreased, pH is decreased, or buffer composition is changed. Observed artifacts include: a diminished anodic peak current following the first reduction wave and appearance of a substance irreversibly oxidized at a potential more positive than $(E_{1/2})_1$ (Figure 2A), a decrease in magnitude of the second peak and appearance of a reversible couple at a potential between $(E_{1/2})_1$ and $(E_{1/2})_2$ (Figure 2B), and a decrease in magnitude of the second peak and appearance of a reversible couple at a potential more negative than $(E_{1/2})_2$ (Figure 2C). These artifacts are the result of chemical reactions occurring after the electron-transfer steps and indicate that the initial electrode products have only transient stability. However, in most circumstances the behavior of Figure 1 can be restored by increasing the sweep rate ($\nu > 0.1$ V s^{-1}), thereby making it possible to determine the electrode half-reactions from shifts of $E_{1/2}$ with solution conditions.

The half-wave potentials of both waves vary linearly with pH over the range pH 3.5–7 in buffers of acetate, formate, phosphate, and pyridine (when corrected for py coordination,

(30) W. E. Newton and J. W. McDonald, *J. Less-Common Met.*, **54**, 51 (1977).
(31) R. Weinland and P. Huthmann, *Arch. Pharm. Ber. Dtsch. Pharm. Ges.*, **262**, 329 (1924); R. Weinland, A. Babel, K. Gross, and H. Mai, *Z. Anorg. Allg. Chem.*, **150**, 177 (1926).
(32) R. S. Nicholson and I. Shain, *Anal. Chem.*, **36**, 706 (1964).
(33) D. S. Polcyn and I. Shain, *Anal. Chem.*, **38**, 370 (1966).

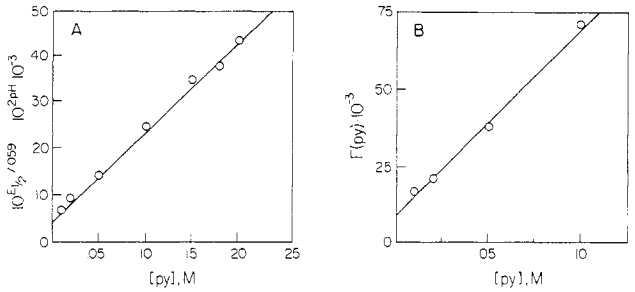

Figure 3. Plots of voltammetric half-wave potential data to determine equilibrium constants for pyridine coordination in (A) Mo(V) product and (B) Mo(III) product.

vide infra). Data from all four buffer systems fit the relationships $(E_{1/2})_1 = +0.206 - 0.116(\mathrm{pH})$ and $(E_{1/2})_2 = -0.547 - 0.058(\mathrm{pH})$. No shift is observed in either $E_{1/2}$ if the concentration of catechol (0.015–0.15 M) or molybdenum(VI) (0.1–2.0 mM) is varied. Thus, the two half-reactions for $MoO_2(cat)_2^{2-}$ reduction may be written as

$$MoO_2(cat)_2^{2-} + 2H^+ + e^- \rightleftarrows MoO(H_2O)(cat)_2^- \quad (E_{1/2})_1 \tag{3}$$

$$MoO(H_2O)(cat)_2^- + 2H^+ + 2e^- \rightleftarrows Mo(H_2O)_2(cat)_2^- \quad (E_{1/2})_2 \tag{4}$$

Pyridine Coordination. In pyridine buffers the half-wave potentials of both waves vary with pyridine concentration at constant pH. The changes are in the direction of py coordination to the electrode products. For the first wave the change in $(E_{1/2})_1$ with log [py] is nonlinear and less than the +59 mV per decade slope expected if the Mo(V) product were quantitatively coordinated by one molecule of pyridine. The data are treated in terms of partial coordination according to eq

$$MoO(H_2O)(cat)_2^- + py \rightleftarrows MoO(py)(cat)_2^- + H_2O \quad \beta_1{}^{V}{}_{py} \tag{5}$$

5 in conjunction with electrode reaction 3. The expression for the half-wave potential is

$$(E_{1/2})_1 = (E_{1/2})_1' - 0.118(\mathrm{pH}) + 0.059 \log (1 + \beta_1{}^{V}{}_{py}[py]) \tag{6}$$

where $(E_{1/2})_1'$ is the half-wave potential of reaction 3 at pH 0 and $\beta_1{}^{V}{}_{py}$ is the formation constant of the mono(pyridine) adduct of the molybdenum(V)–catechol complex. Data from seven pH 4.7–6.7 pyridine buffer solutions are plotted antilogarithmically in Figure 3A according to eq 7. The slope and intercept yield $\beta_1{}^{V}{}_{py} = 40 \pm 20\ M^{-1}$ and $(E_{1/2})_1' = +0.22 \pm 0.01$ V vs. SCE.

$$10^{(E_{1/2})_1/0.059}10^{2(\mathrm{pH})} = 10^{(E_{1/2})_1'/0.059} + 10^{(E_{1/2})_1'/0.059}\beta_1{}^{V}{}_{py}[py] \tag{7}$$

The effect of pyridine coordination on the second reduction step is treated by considering equilibria 8 and 9 in conjunction

$$Mo(H_2O)_2(cat)_2^- + py \rightleftarrows Mo(H_2O)(py)(cat)_2^- + H_2O \quad \beta_1{}^{III}{}_{py} \tag{8}$$

$$Mo(H_2O)_2(cat)_2^- + 2py \rightleftarrows Mo(py)_2(cat)_2^- + 2H_2O \quad \beta_2{}^{III}{}_{py} \tag{9}$$

with electrode reaction 4. Following the principles of DeFord and Hume[34] for consecutive complexation reactions, the term $F(py)$ is defined.

$$F(py) = \beta_1{}^{III}{}_{py} + \beta_2{}^{III}{}_{py}[py] \tag{10}$$

(34) D. D. DeFord and D. N. Hume, *J. Am. Chem. Soc.*, 73, 5321 (1951).

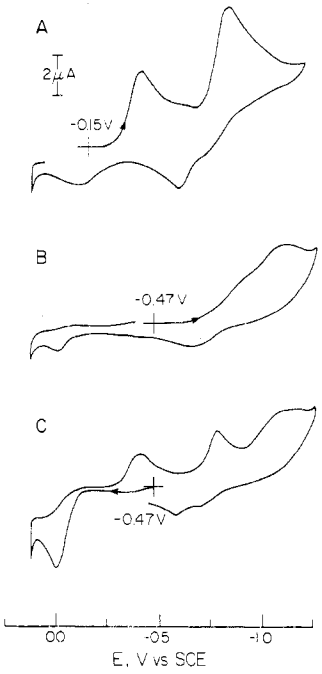

Figure 4. Cyclic voltammograms of $MoO_2(cat)_2^{2-}$ before and after coulometric reduction by one electron in pyridine buffer (1.25 mM Mo(VI), 0.15 M H_2cat, 0.1 M pyH^+, 0.1 M py, pH 5.7, sweep rate = 0.05 V s^{-1}): (A) $MoO_2(cat)_2^{2-}$, (B) negative-going scan after reduction, (C) positive-going scan after reduction.

Recalling that the Mo(V) electrode product is partially coordinated by pyridine and applying material balance considerations, we calculated $F(py)$ from experimental quantities using the relationship

$$F(py) = \frac{(1 + \beta_1{}^{V}{}_{py}[py])10^{|(E_{1/2})_2 - (E_{1/2})_2''|/0.0296} - 1}{[py]} \tag{11}$$

$(E_{1/2})_2''$ is the half-wave potential of reaction 4 in noncoordinating buffers at the (constant) pH of the experiment. $F(py)$ is plotted against [py] in Figure 3B for a series of pH 5.70 pyridine buffers. Values of $\beta_1{}^{III}{}_{py} = (1.0 \pm 0.7) \times 10^4\ M^{-1}$ and $\beta_2{}^{III}{}_{py} = (6.1 \pm 1.3) \times 10^5\ M^{-2}$ are obtained for formation constants of the mono- and bis(pyridine) adducts of the molybdenum(III)–catechol complex.

Molybdenum(V) Dimerization. The one-electron reduction product of $MoO_2(cat)_2^{2-}$ is not stable at pH <7. Voltammograms of a solution coulometrically reduced at $(E_{1/2})_2 < E < (E_{1/2})_1$ show neither of the original redox couples (Figure 4). Rather, a broad, irreversible reduction is observed at −1.1 V on negative-going scans (Figure 4B), and a well-defined, irreversible oxidation at 0.0 V on positive-going scans (Figure 4C). Sweep reversal after the oxidation wave produces reduction peaks at potentials corresponding to the original Mo(VI)/Mo(V) and Mo(V)/Mo(III) couples. Coulometric reoxidation of the Mo(V) solution at +0.08 V consumes 0.97 faradays/mol of molybdenum and quantitatively regenerates the original voltammogram shown in Figure 4A. The foregoing results occur identically in pyridine and phosphate buffers.

The amber color of the electrolyzed solutions and the prevalence of di-μ-oxo dimers of this color in Mo(V) chemistry suggest that the coulometric reduction product could be such a binuclear species. Attempts to isolate the electrochemically generated material were unsuccessful due to difficulties arising from catechol oxidation during workup of the solutions. However, the compound $BaMo_2O_4(cat)_2(H_2O)_2$ was readily prepared and characterized as described in the Experimental Section. Addition of this compound to pH 5.7 pyridine buffer

Table II. Kinetics of Mo(V) Dimerization in Pyridine Buffer[a]

$10^3[MoO_2(cat)_2^{2-}]$, M	[py], M	[H_2cat], M	pH	i_{pa}/i_{pc}[b]	k_{obsd}[c] M^{-1} s^{-1}
1.00	0.01	0.15	5.71	0.728	80
1.02	0.02	0.15	5.67	0.729	63
1.01	0.05	0.15	5.67	0.818	35
1.01	0.10	0.15	5.65	0.889	19
0.98	0.20	0.15	5.61	0.937	11
1.04	0.10	0.15	6.65	0.931	10
1.06	0.10	0.15	6.26	0.920	12
1.01	0.10	0.15	5.93	0.893	19
1.02	0.10	0.15	5.32	0.811	38
1.00	0.18	0.015	6.56	0.753	66
1.00	0.18	0.03	6.56	0.790	48
1.00	0.18	0.06	6.56	0.874	21
1.00	0.18	0.10	6.56	0.922	12
0.15	0.10	0.15	5.46	0.982	25
0.38	0.10	0.15	5.46	0.967	18
1.05	0.10	0.15	5.46	0.888	28
1.55	0.10	0.15	5.46	0.850	22
1.95	0.10	0.15	5.46	0.835	21

[a] $\mu = 0.5(Na_2SO_4)$; 25 °C. [b] Average of two or more trials at $\nu = 0.01$ V s^{-1}. [c] From working curve of (i_{pa}/i_{pc}) vs. log ($k_{obsd}C\tau$) and corrected for spherical diffusion as described in ref 35.

(with sodium sulfate added to precipitate barium ion) produces voltammetric traces which match those in Figure 4B, C in all respects. Thus, the molybdenum(V)–catechol electrode product dimerizes according to the stoichiometry

$$2MoO(H_2O)(cat)_2^- \rightarrow Mo_2O_4(cat)_2(H_2O)_2^{2-} + 2H_2cat \quad (12)$$

The kinetics of this reaction in pyridine buffers were investigated by cyclic voltammetry using the theory of Olmstead et al.[35] for an irreversible dimerization following a reversible charge transfer. The voltammogram in Figure 2A shows the decrease in anodic peak current of the Mo(V) monomer and appearance of an oxidation wave for Mo(V) dimer resulting from this reaction at slow sweep rates. An observed second-order rate constant for the reaction was calculated from anodic-to-cathodic peak current ratios of the Mo(VI)/Mo(V) monomer wave and working curves constructed from the data in ref 35. The results in Table II illustrate that i_{pa}/i_{pc}, but not k_{obsd}, depends on molybdenum concentration, as expected for a second-order process. In addition, the observed rate constant increases with decreasing pyridine concentration, decreasing catechol concentration, and increasing acidity. These relationships are plotted in Figure 5.

A mechanism for Mo(V) dimerization consistent with the experimental results consists of reactions 3 and 5 followed by

$$MoO(H_2O)(cat)_2^- + 2H_2O \rightleftarrows MoO(OH)_2(H_2O)(cat)^- + H_2cat \quad 1/K_2^{V}_{cat} \quad (13)$$

$$2MoO(OH)_2(H_2O)(cat)^- \xrightarrow{k_2} Mo_2O_4(cat)_2(H_2O)_2^{2-} + 2H_2O \quad (14)$$

$$2MoO(OH)_2(H_2O)(cat)^- + H^+ \xrightarrow{k_3} Mo_2O_4(cat)_2(H_2O)_2^{2-} + H_3O^+ + H_2O \quad (15)$$

The observed rate constant is given by

$$k_{obsd} = \frac{k_2 + k_3[H^+]}{1 + K_2^{V}_{cat}[H_2cat](1 + \beta_1^{V}_{py}[py])} \simeq \frac{k_2 + k_3[H^+]}{K_2^{V}_{cat}[H_2cat](1 + \beta_1^{V}_{py}[py])} \quad (16)$$

(35) M. L. Olmstead, R. G. Hamilton, and R. S. Nicholson, *Anal. Chem.*, **41**, 260 (1969).

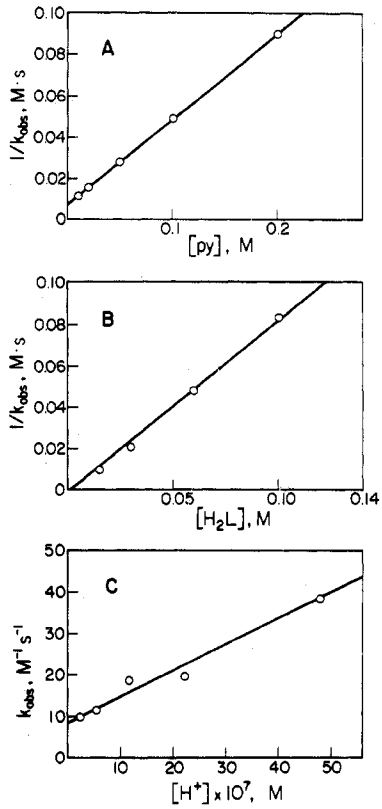

Figure 5. Plots of the observed rate constant for Mo(V) dimerization as a function of (A) pyridine concentration, (B) catechol concentration, and (C) hydrogen ion concentration.

Starting with $MoO(py)(cat)_2^-$ the mechanism proceeds by dissociation of one molecule of pyridine and one molecule of catechol to produce, as a reactive intermediate, the 1:1 Mo(V)–catechol monomer formulated here as $MoO(OH)_2(H_2O)(cat)^-$. The species undergoes dimerization via acid-independent and acid-dependent pathways in the rate-determining reactions 14 and 15. By use of the plot of $1/k_{obsd}$ vs. [py] in Figure 5A and the approximate form of eq 16, a value of $\beta_1^{V}_{py} = 55 \pm 15$ M^{-1} is obtained, in satisfactory agreement with the result of 40 M^{-1} from half-wave potential measurements. $1/K_2^{V}_{cat}$ represents the equilibrium constant for dissociation of one catechol molecule from the bis(catechol)–Mo(V) monomer. The near-zero intercept of the $1/k_{obsd}$ vs. [H_2cat] plot in Figure 5B indicates that the equilibrium in reaction 13 lies far to the left and leads to the approximation $K_2^{V}_{cat}[H_2cat](1 + \beta_1^{V}_{py}[py]) \gg 1$ in eq 16. This result is consistent with the supposition that $MoO(OH)_2(H_2O)(cat)^-$ is the reactive intermediate in the system. Insufficient data were taken to evaluate $K_2^{V}_{cat}$, k_2, and k_3. However, from the results in Figure 5C the ratios $k_3/k_2 = 7 \times 10^6$ M^{-1} s^{-1} and $k_2/K_2^{V}_{cat} = 8$ s^{-1} can be calculated. In the plot of $1/k_{obsd}$ vs. [H_2cat] in Figure 5B, the slope is 0.83 s, and the intercept is <0.001 M·s; thus, $K_2^{V}_{cat} > 800$ M^{-1}. This result is consistent with the observation for the molybdenum(VI)–catechol complex[18] that $K_2^{VI}_{cat} = \beta_2^{VI}/\beta_1^{VI} = 1.5 \times 10^3$ M^{-1}. Therefore, limits can be established for the dimerization rate constants of $k_2 > 6.4 \times 10^3$ M^{-1} s^{-1} and $k_3 > 4.5 \times 10^{10}$ M^{-2} s^{-1}.

Discussion

A summary of the electrochemical behavior of $MoO_2(cat)_2^{2-}$ in weakly acidic buffer solutions is presented in Figure 6. Uptake of two protons accompanies each electron-transfer step and converts an oxo group to a coordinated water molecule. The aquo groups are labile and can either be replaced by a suitable complexing agent (e.g., pyridine) in the Mo(V) and Mo(III) states or undergo dimerization in the Mo(V) state.

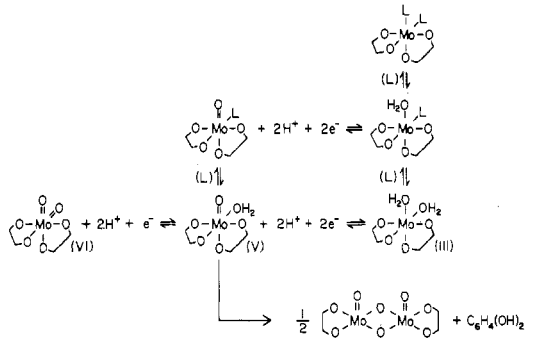

Figure 6. Summary of electrochemical behavior of molybdenum catechol complexes at pH 3.5–7. L = pyridine.

Under the experimental conditions of [py] = 0.01–0.20 M, it is calculated that 33–90% of the Mo(V) monomer exists as the mono(pyridine) adduct and 32–98% of the Mo(III) monomer as the bis(pyridine) adduct. Thus, substitution of pyridine at the aquo coordination sites is incomplete. As a result of this incomplete substitution and the labile nature of eq 5, reactions 13–15 shift in the direction of dimer formation following reduction to molybdenum(V).

Zelinka, Bartusek, and Okac[27] previously determined the electron and proton stoichiometries of $MoO_2(cat)_2^{2-}$ reduction by polarography. These authors suggested that $Mo(OH)_2(cat)_2^-$ is the initial electrode product and is converted by a slow chemical reaction to the less easily oxidized species $MoO(H_2O)(cat)_2^-$. However, our results establish that the latter species is produced initially and undergoes dimerization to $Mo_2O_4(cat)_2(H_2O)_2^{2-}$, which is the substance oxidized at a potential more positive than $(E_{1/2})_1$. Identification of $MoO(H_2O)(cat)_2^-$ as the primary electrode product is consistent with the almost ubiquitous presence of the Mo=O functional group in Mo(V) chemistry.[36] Production of a $Mo_2O_4^{2+}$ dimer containing one terminal oxo group per molybdenum and the ability to coordinate no more than one pyridine molecule after the first reduction step constitute proof that the Mo=O functionality is retained upon reduction to the Mo(V) state. Zelinka et al. also attributed the shift in $(E_{1/2})_1$ with total pyridine buffer concentration to formation of an ion pair between $Mo(OH)_2(cat)_2^-$ and pyridinium ion.[27] However, when changes in pH are accounted for in buffers of varying composition, it is apparent that the shift in $(E_{1/2})_1$ results from py coordination and not pyH^+ ion-pair formation. Thus, the scheme in Figure 6 is presented as the correct interpretation of $MoO_2(cat)_2^{2-}$ electrochemistry.

Catechol is unique in its ability to promote reversible electron transfer among monomeric Mo(VI), -(V), and -(III) species in aqueous media. The electron donating/accepting properties of the aromatic ligand presumably are responsible in part for this behavior. However, as is shown in EPR experiments on the Mo(V) monomer,[28] the unpaired electron is localized largely on the metal and not the ligand. The analogous tungsten(VI) complex, $WO_2(cat)_2^{2-}$, undergoes one-electron reduction at −1.16 V in pH 6.7 pyridine buffer.[37] This potential is 0.6 V more negative than for $MoO_2(cat)_2^{2-}$ reduction under the same conditions, and the large difference strongly suggests metal-centered electron transfer in these complexes.

Another feature of $MoO_2(cat)_2^{2-}$ redox behavior is the reversible interconversion of oxo and aquo groups during the oxidation and reduction steps. Similar behavior is notably absent in the aqueous electrochemistry of *fac*-trioxo MoO_3L species,[38] where complicated, irreversible behavior generally is observed, and in the nonaqueous electrochemistry of *cis*-dioxo MoO_2L_2 species,[3,7,39] where (often irreversible) one-electron transfer prevails. A greater parallel exists with the electrochemistry of the dimeric molybdenum(V) complexes, $Mo_2O_2X_2(L\text{-}L)^{2-}$ (X_2 = μ-O_2, μ-OS, μ-S_2; (L-L) = EDTA, $(cysteine)_2$), in aqueous media.[1,2,4] In both cases Mo(V) → Mo(III) reduction occurs, and the single oxo group on Mo(V) is converted to aquomolybdenum(III) (frequently being replaced by a coordinating buffer molecule). The molybdenum(IV) oxidation state is bypassed in both instances. One implication[16] of this result is that the Mo(IV) state has special structural requirements which make it inaccessible from the oxomolybdenum(V) and aquomolybdenum(III) species studied in these experiments.

The ability to reversibly generate molybdenum(V) catechol monomer has enabled for the first time a comprehensive study of molybdenum(V) dimerization kinetics. The mechanism outlined in reactions 13–15 requires dissociation of one molecule of catechol in addition to pyridine prior to the rate-determining step. Therefore, we postulate that more than one nonligated site (aquo or hydroxo group excluded) is required for formation of the di-μ-oxo dimer. In an earlier study of Mo(V) dimerization in tartrate media, Spence and Heydanek[40] observed similar increases in the rate of dimerization with increasing acidity and decreasing buffer concentration. The rate constant in tartrate buffer is ca. 5 times greater than that for the catechol system under approximately equivalent conditions. These similarities suggest the possibility that the mechanism proposed in reactions 13–15 is generally applicable to oxomolybdenum(V) → $Mo_2O_4^{2+}$ dimerization.

Spence[40] and Haight and co-workers[41] have detected small quantities of Mo(V) monomer in equilibrium with $Mo_2O_4^{2+}$ dimers by EPR spectroscopy. In several instances following coulometric reduction of $MoO_2(cat)_2^{2-}$ in pyridine and phosphate buffers, we have observed small (~6% of total molybdenum) voltammetric peaks which correspond to the monomeric Mo(VI)/Mo(V) catechol couple. We have not attempted to ascertain whether this result signifies occasionally incomplete reduction of Mo(VI) or a small fraction of Mo(V) monomer in equilibrium with $Mo(V)_2$. However, if the latter possibility is the case, reaction 12 should be represented as a reversible equilibrium largely displaced to the right. In view of results presented in our subsequent paper concerning production of stable monomeric species in alkaline media,[28] the question of possible dimer ⇄ monomer equilibrium in the molybdenum(V)–catechol system deserves further study.

Acknowledgment. Support of this research by the National Science Foundation under Grant No. CHE 76-18703 is gratefully acknowledged.

Registry No. $MoO_2(cat)_2^{2-}$, 72985-79-6; $MoO(H_2O)(cat)_2^-$, 73037-33-9; $Mo(H_2O)_2(cat)_2^-$, 72985-78-5; $MoO(py)(cat)_2^-$, 72985-77-4; $Mo(H_2O)(py)(cat)_2^-$, 72985-76-3; $Mo(py)_2(cat)_2^-$, 72985-75-2; $Mo_2O_4(cat)_2(H_2O)_2^{2-}$, 72985-74-1; $BaMo_2O_4(cat)_2(H_2O)_2$, 72985-73-0; sodium molybdate, 7631-95-0.

(36) E. I. Stiefel, *Prog. Inorg. Chem.*, **22**, 1 (1977).
(37) L. M. Charney and F. A. Schultz, unpublished work.
(38) F. A. Schultz and D. T. Sawyer, *J. Electroanal. Chem.*, **17**, 207 (1968).
(39) A. F. Isbell, Jr., and D. T. Sawyer, *Inorg. Chem.*, **10**, 2449 (1971).
(40) J. T. Spence and M. Heydanek, *Inorg. Chem.*, **6**, 1489 (1967).
(41) T. J. Huang and G. P. Haight, Jr., *J. Am. Chem. Soc.*, **92**, 2336 (1970); **93**, 611 (1971); T. Imamura, G. P. Haight, Jr., and R. L. Belford, *Inorg. Chem.*, **15**, 1047 (1976); G. P. Haight, G. Woltermann, T. Imamura, and P. Hummel, *J. Less-Common Met.*, **54**, 121 (1977).